X-ray polarimetry small satellite TSUBAME

Takahiro Toizumi[1], Takeshi Nakamori[1], Jun Kataoka[1], Yoshihiro Tsubuku[1],
Yoichi Yatsu[1], Makoto Arimoto[1], Takashi Shimokawabe[1], Nobuyuki Kawai[1],
Kuniyuki Omagari[2], Hiroki Ashida[2], Saburo Matsunaga[2] et al.

[1] Department of Physics, Faculty of Science, Tokyo Tech, Meguro, Tokyo, Japan
[2] Department of Mechanical and Aerospace Engineering, Tokyo Tech, Meguro, Tokyo, Japan
E-mail(TT): toizumi@hp.phy.titech.ac.jp

ABSTRACT

TSUBAME is a university-built small satellite mission to measure polarization of hard X-ray photons (30-100 keV) from Gamma-ray bursts (GRBs) using azimuthal angle anisotropy of Compton-scattered photons. Polarimetry in the hard X-ray and soft γ-ray band plays a crucial role in the understanding of high energy emission mechanisms and the distribution of magnetic fields and radiation fields. TSUBAME has two instruments: the Wide-field Bust Monitor (WBM) and the Hard X-ray Compton Polarimeter (HXCP). The WBM determines on board the direction of the burst occurrence with an accuracy of 10 degrees, then using a high speed attitude control device, the HXCP is pointed to the GRB within 15 seconds after the burst occurrence to promptly detect polarized X-ray photons from the GRB.

KEY WORDS: gamma-ray bursts — Polarimetery

1. Introduction

In the study of GRBs and other X-ray and γ-ray sources, analyses of their spectra and time variability are common. But the information extracted from these observations may not be sufficient to identify the dominant emission mechanism. In some cases, measurements of thepolarization can clarify the emission mechanism and the orientation of the polarization plane will provide an idea of the distribution of magnetic field, radiation field and matter around the sources such as rotation powered pulsars, accreting black holes and AGNs. The reliable polarimetry in X-ray band has been done only once at the energies 2.6 and 5.2 keV using Bragg reflection [1]. Furthermore, for GRBs, only a few observations of X-ray polarimetry has been done [2], and these results were disputable because of a low level of significance [3]. In such situations, new observatories having a high sensitivity of X-ray polarimetry for GRBs have been long-awaited.

2. TSUBAME Mission Overview

TSUBAME, meaning a bird swallow in Japanese, is a small satellite that will measure the polarization of astronomical objects. The dimensions of TSUBAME are $300 \text{ mm} \times 300 \text{ mm} \times 300 \text{ mm}$ and the total mass is ~ 30 kg. TSUBAME is planned to be launched as a piggyback on the HIIA rocket. The main target of TSUBAME is GRBs. A rapid observation in the study of GRBs is needed because the duration of prompt emission is generally short ($2 \sim 100$ sec). A schematic observation sequence is shown in Fig. 1, when a GRB occurs, TSUBAME localizes the coordinates of the GRB on board using the localization detector WBM. By slewing promptly using the rapid maneuvered system (~ 90 deg within 15 sec), the HXCP is pointed to the position of the GRB and starts the observation in 15 s after the burst occurrence. The WBM consists of 5 sets of a CsI scintillator connected to APDs. These CsI scintillators are attached to each corner of the observatory, shown in Fig. 2. Using the count rates of 5 detectors, GRBs will be localized with an accuracy of ~ 10 degrees. FOV of the WBM is 2π str (half of the whole sky).

1. Burst occurence

2. Detection and localization

3. High-speed attitude maneuver
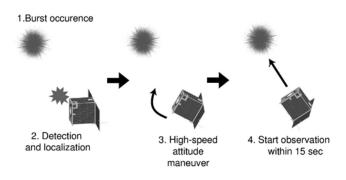
4. Start observation within 15 sec

Fig. 1. TSUBAME observation sequence.

The polarimeter HXCP will measure the polarized photons in the $30 \sim 200$ keV band using the azimuthal angle anisotropy of Compton scattered photons, and consists of 8×8 plastic scintillators (scatterers) connected

to a MAPMT R8900-M16-UBA and 36 CsI scintillators (absorbers), each connected to an APD S8664-55 [5] surrounding the 8 × 8 scatterers, shown in Fig. 2. The effective area is ∼ 5 cm² and its field of view is 25 deg².

Now we assume to mount two HXCPs in TSUBAME. One with a collimator and the other without a collimator. The HXCP without collimator has large field of view but the background level is high, another HXCP with a collimator has lower background level but narrow field of view. TSUBAME aims to detect polarization from not only GRBs but also bright galactic diffuse sources (e.g., Crab Nebula), binary systems (e.g., Cyg X-1) and flares from blazars or soft gamma-ray repeaters. If the objects are very bright (≥ 1 Crab), TSUBAME can detect the polarization from these objects significantly with the HXCP with a collimator.
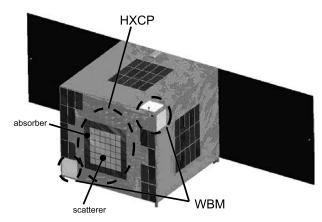

Fig. 2. TSUBAME configuration. HXCP is centered at the observatory. The HXCP consists of 8 × 8 plastic scintillators as a scattering site and 32 CsI scintillators as a photoelectric absorption site surrounding scatteres. Counters of the WBM are attached to each corner of the observatory.

3. HXCP Simulation

We performed a Compton simulation to determine the signal and background levels of HXCP, using Geant4 and the detectability of the polarization from GRBs. We use a modulation factor as a indicator of the performance of HXCP. Modulation factor is defined as the relative amplitude of te modulation curve (i.e. number of Compton-scattered phton s as a function of the azimuthal scatter angle) for 100 % polarized photons.

3.1. GRB021206

We simulate a GRB event; GRB 021206 which had a flux of 3.2×10^{-5} ergs/cm²/s and a duration of 5.5 s. This event was a very bright GRB for which a strong polarization was reported(Coburn et al. 2003).

In this simulation, we assume that the burst photons are 100 % polarized and the energy range is 30 ∼ 200 keV. Here, the dominant γ-ray background are CXB and atmospheric γ-ray. The γ-ray background flux models have been developed based on observation data(Mizuno et al. 2004) and we generate the CXB and atmospheric γ-ray, representative of the satellite environment. We find that the background induced by high-energy charged particles can be easily rejected because the charged particles deposit very large signals(out of energy range) through the scintillators.

3.2. Design study

We optimized the design of the HXCP scintillators, i.e. number, pixel size and length of scintillators. To determine these parameters, we obtained the value of the modulation factor (MF), the effective area, and the minimum detectable polarization (MDP) by simulations. In conclusion, we obtained a best result with a plastic scintillator array of 64 pixels, CsI scintillator of 32 pixels, and the pixel size of the plastic scintillator of 7.5 mm × 7.5 mm, and the length of the scintillator of 50 mm. The effective area is, then, ∼5 cm², the MF is 47.6 ± 1.2 %, the MDP is 8.1 %. One of the simulation results are shown in Fig. 4 and Fig. 5. Fig. 4 shows the spectra of incident GRB photons, the Compton scattered photons detected, and the background.
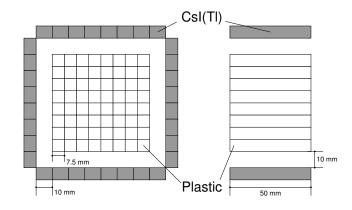

Fig. 3. Detctor design of HXCP(left: top view, right : side view)

3.3. Fine collimator

A fine collimator can improve the dtection efficiency for the polarization. in the previous section, scintillator design is fixed to the optimum value. Using this value, the fine collimator design was optimized. We obtained that the best collimator lenngth is 55 mm, tickness is 500 μm and the number of collimator grid is 4 × 4 or 8 × 8. With this collimator, we can make the polarimetry of the Crab Nebula wiht MDP ≤ 20 %.

4. Development of photon detector for scatterer

4.1. Performance of malti anode PMT (MAPMT) of UBA

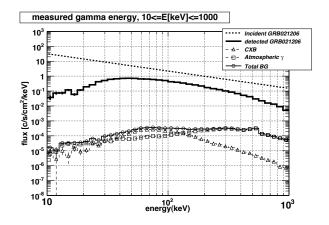In the TUSBAME mission, the MAPMTs are used to detect the position where the Compton scattering occurs.

Fig. 4. Spectrum of GRB021206. Energy vs. flux. Energy range is 30 ∼ 200 keV. The flux of GRB021206 is more significant than total background.
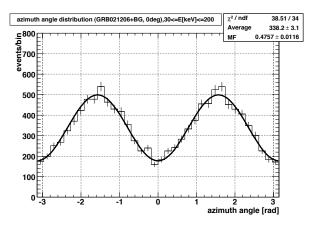

Fig. 5. Aimuthal modulation curve of GRB021206. MF = 47.6 %, MDP = 8.1 %.

These MAPMTs reuires high sensitivity for scintillation phtons because the light yield of the plastic scintillator of HXCP is low (5 photons/keV). In addition, it is necessary to apply a vibration test to them before the launch.

MAPMT-R8900-M16-UBA has 16 anodes and ultra bialkali (UBA) photo cathode. It is compact and require low voltage (∼ 800 V) compared to other PMTs (∼ 1500 V). The quantum efficiency of UBAs is more than 40 %, doubled form the bialkari (BAs). Although it is usually diffcult to become rugged for vibration because the configuration of dynodes is complicated, with HPK(Hamamatsu Photonics K.K.), we have developed the raggedness to survive.

4.2. Spectrum of ^{241}Am and single photoelectron

Fig.7 shows the spectrum irradiated with a ^{241}Am source γ-ray photons obtained with the MAPMT-R8900-M16-UBA and plastic scintillators. In this spectrum, we can cleanly see not only the 59.5 keV peak but also a lower energy peak (∼ 20 keV).
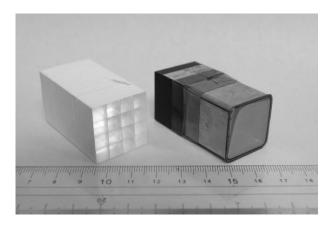
Fig.8 shows the spectrum of single photoelectrons.

Fig. 6. MAPMT-R8900-M16-UBA and 16 pixel plastic scintillator array.

Single photoelectron peak corresponds to 0.96 keV by comparing with the 59.5 keV peak in the spectrum of ^{241}Am.
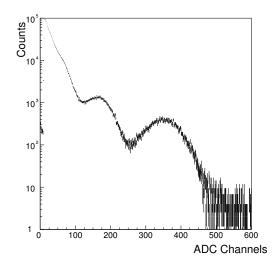

Fig. 7. The spectrum of ^{241}Am by the plastic scintilator and the MAPMT with UBA. This spectrum shows not only 59.5 keV peak but also lower energy peak. At 59.5 keV peak, energy resolution is 29.9 %.

4.3. UBA performance for polarimeter

By improving the quantum efficiency of MAPMT, it becomes possible to detect the low energy (≥ 0.96 keV) Compton scatterings photons in the plastic sintillators. This is a significant improved over BA, which show single photoelectron peak of 2.7 keV. With this improvement, we shold be able to detect Compton scattering with small energy deposit. That is, number of events for the polarized X-ray detection increase, and the possibility that the polarization can be detected rises.
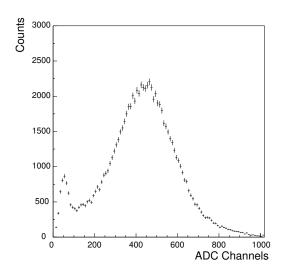
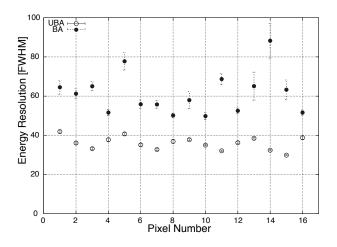Fig. 8. The spetrum of single photoelectron. ADC channel vs. Counts.

Fig. 9. Deference of energy resolution comparing UBA with BA. UBA has better resolution than BA in all pixels. Anode pixel number vs. energy resolution.

4.4. Vibration test

Standard MAPMTs lack improved tolerance and are not completely reliable against vibration impact when launching a rocket. The R8900-200-M16MOD-UBA offers improved tolerance to vibration in possible launching vehicles. Prior to delivering the MAPMTs to us, Hamamatsu Photonics K.K. tested 10 samples units using random levels of vibration up to 15 G_{rms}, and a shock level of 60 G. We continued detailed vibration testing on each MAPMT to confirm tolerance to random vibration that is 1.5 times that of the HIIA profile and determine the maximum vibration that each unit can withstand. The dynode represents the weak point relative to vibration. When the dynode is damaged, the MAPMT loses gain. Therefore, we examined variations in gain caused by vi-

bration. In testing vibration for the MAPMT, we used a vibration generator (IMV i230/SA2M). The frequency profile was random vibration based on the HIIA profile as listed in Table 1. Random vibration was applied to three axes (X, Y, and Z). The duration of vibration for each axis was two minutes.

We initially tested at 12 G_{rms}. Before and after this test, we examined the MAPMT gain by using single photoelectron spectra.

We then accelerated the vibration and examined the gain after each test. Vibration was accelerated from 5 G_{rms} to 17 G_{rms} in increments of 3 G_{rms}. After vibratin at 12 and 17 G_{rms}, no significant change in signal output was noted. Therefore, The MAPMT was considered to withstand vibration even at double the conditions of the HIIA rocket profile.

Table 1. Characteristics of the frequency profile used in the vibration test. The duration of vibration was 120 sec.

Frequency range(Hz)	Vibration profile
20 ~ 200	+3.0 dB/oct
200 ~ 2000	0.032 G^2/Hz (for 7.8 G_{rms})

5. Future Plan for TSUBAME

We plan to estimate the performance of the prototype of the HXCP includeing plastic scintillators coupled MAPMTs and CsI scintillators coupled to APDs using a synchrotron X-ray beam line. In addition to WBM to localize GRBs position, we need to estimate its localization ability using Monte Carlo simulating. Based on the optimized the design, we will develop the engineering model of WBM.

References

[1] Weisskopf, M. C., et al. 1976, ApJL, 208, L125
[2] Coburn, W. & Boggs, S. E. et al. 2003, Nature, 423, 415
[3] McGlynn, S., et al. 2007, A&A, 466, 895
[4] Ikagawa, T., et al. 2003, NIMA, 515, 671
[5] Mizuno, T. et al. 2004, Apj, 614, 1113
[6] Kawasaki, Y. et al. 2006, NIMA, 564, 378
[7] Arimoto, M. et al. 2007, AIP, Proceedings of the Santa Fe Conference pp. 607